Closed Loop Model-Based Design of Experiments for Kinetic Model Discrimination and Parameter Estimation: Benzoic Acid Esterification on Heterogeneous Catalyst

Conor Waldron, Arun Pankajakshan, Marco Quaglio, Enhong Cao, Federico Galvanin, Asterios Gavriilidis*

Department of Chemical Engineering, University College London, London WC1E 7JE, UK

*Corresponding author, email address a.gavriilidis@ucl.ac.uk

Abstract

An autonomous reactor platform was developed to rapidly identify a kinetic model for the esterification of benzoic acid and ethanol with the heterogeneous Amberlyst-15 catalyst. A five-step methodology for kinetic studies was employed to systematically reduce the number of experiments required to identify a practical kinetic model. This included i) initial screening using traditional factorial designed steady-state experiments, ii) proposing and testing candidate kinetic models, iii) performing an identifiability analysis to reject models whose model parameters cannot be estimated for a given experimental budget, iv) performing online Model-Based Design of Experiments (MBDoE) for model discrimination to identify the best model from a list of candidates and v) performing online MBDoE for improving parameter precision for the chosen model. This methodology, combined with the reactor platform which conducted all kinetic experiments unattended, reduces the number of experiments and time required to identify kinetic models, significantly increasing lab productivity.

Keywords: automation; closed loop; kinetics; heterogeneous catalysis; flow reactor; string reactor

1. Introduction

Heterogeneous catalysts are of great value to a wide variety of chemical industries including petrochemicals, agrochemicals, bulk chemical production, emission control and the pharmaceutical industries, with some reports estimating that catalysts are involved in the production of over 75% of all chemical products[1]. It is also clear that in order for the chemicals industry to meet the ever increasing demands to reduce the cost and environmental impact of production that new and improved catalysts will need to be developed, studied and optimised. When studying these new catalysts one of the major tasks will be to develop intrinsic kinetic models, as possessing a kinetic model greatly assists the design of industrial scale reactors and their process control systems, as well as offering mechanistic insight into the reaction chemistry[2]. However, obtaining intrinsic kinetic models for heterogeneous catalytic systems is notoriously difficult due to both experimental and modelling challenges. Experimentally it is often difficult to design a reactor that allows study of intrinsic kinetics without heat and mass transport resistances or non-ideal reactor behaviour. On the modelling side it is difficult to identify the correct kinetic model structure from the large number of similar rate laws which are possible depending on the different reaction mechanisms (e.g., Langmuir-Hinshelwood, Eley Rideal), and then often there are a large number of highly correlated parameters that are difficult to estimate[3]. With all these challenges in mind, it is the objective of this work to provide a methodology for the rapid identification of kinetic models for heterogeneous reactions.

Traditionally kinetic studies have been conducted in batch reactors, as this allows the generation of multiple data points per experiment and because these reactors are flexible and easy to operate[4]. However, recently flow reactors and in particular micro flow reactors are becoming more popular for kinetic studies for a number of reasons including their increased heat and mass transfer[5-7], improved safety[8], and because they are compatible with many forms of online analysis[9-14] and they are easier to automate than batch reactors for performing a large number of sequential experiments at different conditions[15-17]. Automated flow reactors offer great opportunities for conducting rapid kinetic studies, as they can be combined with a variety of design of experiment algorithms in closed loop systems, where the reactor platform designs each experiment based on information collected from previously conducted experiments, all without user supervision. These closed loop systems have already shown much success for “self-optimising” reactors where the reactor platform autonomously finds the optimum operating conditions to maximise or minimise given criteria, such as yield or E-factor[14, 18-29], by using response surfaces and optimisation algorithms, such as the SIMPLEX or SNOBFIT algorithms. Similar closed loop systems can also be used for making kinetic studies more efficient, by using Model-Based Design of Experiments (MBDoE), which designs experiments in the most efficient way possible in order to improve model understanding[3]. The field of MBDoE is well established with numerous simulated or offline case studies[3, 30-34] demonstrating its many advantages, and with recent advances in automation several online applications have also been reported[35-40]. The two most common aims of MBDoE are to design experiments to identify which of two or more candidate models is correct[41-44] and then having chosen a single model, to design experiments that will lead to the highest precision in parameter estimation[3, 45, 46]. In terms of developing kinetic models, a number of papers have reported the online use of these techniques in flow and semi-batch reactors, however, to the best of the authors’ knowledge these have only been applied to homogenous systems (a Diels-Alder reaction[35], C-H activation[47], aromatic substitution[36], esterification[38, 40] and to bioreactors[37]). This work presents the first application of closed loop MBDoE for the identification of a kinetic model for a liquid/solid heterogeneous catalytic system.

Applying online MBDoE to a new system is not always straightforward, especially for an unknown catalytic system. There often is the problem of how to design the first experiments when little or no information is available about the system. Furthermore, using MBDoE to pursue kinetic models which are practically unidentifiable for the given experimental budget, allowable design space and precision of the measurements can be a waste of resources and presents another challenge. This second problem is particularly relevant to heterogeneous catalysts as the common Langmuir-Hinshelwood rate laws have a large number of highly correlated parameters, and where it may be more beneficial to pursue a simpler approximated model which is identifiable instead. Therefore, in this work, a methodology is presented that covers all stages of kinetic modelling, from initial experiments, practical identifiability checks to the application of online MBDoE for model discrimination and parameter precision. This is presented using the case study of the esterification of benzoic acid and ethanol using Amberlyst-15 as a heterogeneous catalyst.

2. Modelling & Experimental Methods

2.1 Background to Modelling and Model-Based Design of Experiments

2.1.1 Modelling & Parameter Estimation

A generic model for describing a heterogeneous catalytic reactor consists of a set of algebraic or differential equations, a vector of N_θ non-measurable parameters $\boldsymbol{\theta}$, input or control variables $\mathbf{u}$ and state variables $\mathbf{x}$, that together can be used to predict the values of measurable outlet variables $\hat{\mathbf{y}}$, as shown in Eq 1.

$$\hat{\mathbf{y}} = \mathbf{f}(\mathbf{x}, \mathbf{u}, \boldsymbol{\theta}) \tag{1}$$

In order to use a model for predicting the behaviour of a system, it is necessary to identify the value of the non-measurable parameters $\boldsymbol{\theta}$. This is achieved by performing parameter estimation using experimental data. If the number of experiments conducted is N_{exp}, and each experiment consists of N_m measurements, then for the ith experiment and the jth measurement the residual ρ_{ij} is defined in Eq 2 as the difference between the model prediction $\hat{y}_{ij}$ and the experimental measurement y_{ij}.

$$\rho_{ij} = y_{ij} - \hat{y}_{ij} \tag{2}$$

In this work, parameters are estimated using the maximisation likelihood approach[48], where values for the non-measurable parameters $\boldsymbol{\theta}$ are found which maximise the log likelihood function, $\Phi(\boldsymbol{\theta})$, shown in Eq 3. These parameter values are then called the Maximum Likelihood Estimate (MLE) values , $\widehat{\boldsymbol{\theta}}$.

$$\max_{\boldsymbol{\theta}}(\ \Phi(\boldsymbol{\theta})\ ) = \max_{\boldsymbol{\theta}} \left(\sum_{i=1}^{N_{exp}} \sum_{j=1}^{N_m} -\frac{1}{2} ln(2\pi) - \frac{1}{2} ln\left(\sigma_{ij}{}^2\right) - \frac{1}{2}\left(\frac{\rho_{ij}}{\sigma_{ij}}\right)^2 \right) \tag{3}$$

It is assumed that: i) the inputs **u** are perfectly controlled; and, ii) all residuals are due to measurement error, which is a Gaussian distribution with mean of 0 and standard deviation of σ_{ij}[3, 48].

2.1.2 Goodness of Fit

The validity of a model can be tested using the 95% χ^2 test to determine if the model adequately fits the experimental data available. A χ^2 value is computed according to Eq 4 and this number is

compared against the 95% reference value obtained from statistical tables for the correct number of degrees of freedom ($DoF = N_{exp} * N_m - N_\theta$).

$$\chi^2 = \sum_{i=1}^{N_{exp}} \sum_{j=1}^{N_m} \left(\frac{\rho_{ij}(\hat{\boldsymbol{\theta}})}{\sigma_{ij}} \right)^2 \tag{4}$$

If the χ^2 value is greater than the reference value this indicates that the data are not compatible with the modelling assumptions.

2.1.3 Parameter Precision and Model Prediction Uncertainty

Parameter estimates have a standard deviation to measure their precision, which describes how close one parameter estimate would be to another if all the experiments were repeated. Parameter precision is quantified from the $N_\theta \times N_\theta$ covariance matrix, $\mathbf{V_\theta}$, which can be approximated (using the first term Taylor expansion) by the inverse of observed Fisher information matrix $\mathbf{H_\theta}$.

$$\mathbf{V_\theta} \cong \mathbf{H_\theta^{-1}} \tag{5}$$

The elements in the Fisher information matrix are calculated using the approximation shown below for the kth lth element, where the term $\frac{\partial \hat{y}_{ij}}{\partial \theta_k}$ is the sensitivity of the model prediction $\hat{y}_{ij}$ with respect to parameter k.

$$[\boldsymbol{H_\theta}]_{\boldsymbol{kl}} \cong \sum_{i}^{N_{exp}} \sum_{j}^{N_m} \frac{1}{\sigma_{ij}^2} \left(\frac{\partial \hat{y}_{ij}}{\partial \theta_k} \frac{\partial \hat{y}_{ij}}{\partial \theta_l} \right) \tag{6}$$

From the covariance matrix the 95% confidence interval for the ith parameter is calculated as the square root of the variance element $v_{\theta,ii}$, obtained from the diagonal of the covariance matrix, multiplied by the student t-value at 95% confidence level for the given number of degrees of freedom, as shown in Eq 7. This represents the interval within which it is expected that 95% of the time, parameter estimates would fall if the parameter estimation problem was repeated again with new experimental data.

$$95\%\ Confidence\ Interval_i = \sqrt{v_{\theta,ii}} * t(95\%, DoF) \quad \text{for i} = 1, \dots, N_\theta \tag{7}$$

The t-value for each parameter is calculated by dividing the parameter estimate by the 95% confidence interval, as shown in Eq 8. If the t-value is high, that means the parameter estimate is reliable, however if the value is low it suggests that the parameter confidence interval may include zero and that the parameter statistically may not exist in the model and it may be dropped[3].

$$t_i = \frac{\hat{\theta}_i}{95\%\ Confidence\ Interval_i} \text{ for i} = 1, \dots, N_\theta \tag{8}$$

With the variance-covariance matrix $\mathbf{V_\theta}$, along with the MLE values $\hat{\boldsymbol{\theta}}$, it is possible to quantify the model response uncertainty, which is the uncertainty in the model prediction due to uncertainty in the model parameters. This is done by generating a large number of possible parameter sets using a multivariate normal distribution which takes into account the correlation between the parameters. Then one experiment, designed at some set of control variables **u**, is simulated for each set of parameters. The model responses for each parameter set are recorded and a graph showing the

observed frequency of each model response can be created; the spread of this frequency distribution indicates the level of model uncertainty. This can be repeated at any set of control variables **u**, to observe how model uncertainty varies within the experimental design space.

2.1.4 Model-Based Design of Experiments for Model Discrimination

MBDoE comprises a set of tools for designing experiments in an optimal way, given the information available from the model and from already conducted experiments[3, 48]. In this work, MBDoE tools are used both for model discrimination and for improving parameter precision. In both cases it is necessary to define the design vector **φ**, which is a subset of the control vector **u**, and consists of the experimental variables which are to be optimised. Allowable ranges for each experimental variable are also defined based on experimental constraints.

MBDoE for model discrimination between two or more candidate models involves using the models and their parameter estimates to assist in designing the optimal experiment for distinguishing between the candidate models' responses. There are a variety of different objective functions that can be used to determine the optimum experimental conditions for a discriminating experiment. The simplest objective function, the Hunter Reiner criterion, is the difference in predicted values between each candidate model[41] and is shown in Eq 9 for the case of two candidate models, where $\hat{\mathbf{y}}_\mathbf{1}$ and $\hat{\mathbf{y}}_\mathbf{1}$ are both $1 \times N_m$ matrices containing all the predicted values for model 1 and model 2 respectively, and **σ** is also a $1 \times N_m$ matrix containing the standard deviation for each measurement.

$$\max_{\boldsymbol{\varphi}}\left(\ \psi_{Hunter}(\boldsymbol{\varphi})\ \right) = \max_{\boldsymbol{\varphi}}\left(\left(\frac{\hat{\mathbf{y}}_\mathbf{1} - \hat{\mathbf{y}}_\mathbf{2}}{\boldsymbol{\sigma}}\right)^2\right) \tag{9}$$

However, this simple method relies entirely on the predicted values of each model without taking into account the uncertainty of the model prediction, which can potentially lead to a non-optimal design of experiments. Uncertainty in model prediction arises due to the fact that the parameter values are never exactly known and that each estimated parameter value has an associated uncertainty affecting the expected model responses. More sophisticated model discriminating criteria, such as the one proposed by Buzzi-Ferraris[42-44] take this into account by finding an optimal design vector **φ,** which maximises the divergence between candidate models, while also minimising the uncertainty of the model predictions. In this work the Buzzi-Ferraris method of model discrimination is adopted, and the information regarding the uncertainty in the parameter distributions is contained in the co-variance matrix which is obtained by preforming parameter estimation with previously conducted experiments. The design criterion assuming the presence of 2 candidate model structures is shown in Eq 10.

$$\max_{\boldsymbol{\varphi}}\left(\ \psi_{Buzzi}(\boldsymbol{\varphi})\ \right) = \max_{\boldsymbol{\varphi}}\left(\left(\hat{\mathbf{y}}_\mathbf{1}(\boldsymbol{\varphi}) - \hat{\mathbf{y}}_\mathbf{2}(\boldsymbol{\varphi})\right)^T \mathbf{S}(\boldsymbol{\varphi})^{-1}\left(\hat{\mathbf{y}}_\mathbf{1}(\boldsymbol{\varphi}) - \hat{\mathbf{y}}_\mathbf{2}(\boldsymbol{\varphi})\right)\right) \tag{10}$$

Here, **S**(**u**) is the total variance due to covariance of the measurement noise **M**, and the covariance of the model predictions of model 1, $\mathbf{P}_1$ and model 2, $\mathbf{P}_2$ as shown in Eq 11.

$$\mathbf{S}(\boldsymbol{\varphi}) = 2\mathbf{M} + \mathbf{P}_1(\boldsymbol{\varphi}) + \mathbf{P}_2(\boldsymbol{\varphi}) \tag{11}$$

The covariance of the measurement noise, **M**, is a $N_m \times N_m$ matrix where the diagonal entries are the standard deviation for each measurement and the off-diagonal entries are 0. The covariance of the model predictions for the kth model, $\mathbf{P_k}$, which is the uncertainty in the model prediction, is in turn calculated from the covariance matrix, $\mathbf{V}_{\theta,k}$, and the sensitivity matrix, $\mathbf{Q_k}(\boldsymbol{\varphi})$, for that model, as shown in Eq 12.

$$\mathbf{P}_k(\boldsymbol{\varphi}) = \mathbf{Q}_k(\boldsymbol{\varphi})\mathbf{V}_{\theta,k}\mathbf{Q}_k^T(\boldsymbol{\varphi}) \quad \text{for k } = 1 \text{ and } 2 \tag{12}$$

The i,jth element of the sensitivity matrix $\mathbf{Q_k}(\boldsymbol{\varphi})$ is the partial derivative of the kth model prediction for the ith model response variable with respect to parameter j at conditions $\boldsymbol{\varphi}$.

$$\mathbf{Q}_k(\boldsymbol{\varphi}) = \frac{\partial \hat{y}_{i,k}}{\partial \theta_j}_{\,at\ conditions\ \boldsymbol{\varphi}} \tag{13}$$

The importance of using a model discrimination objective function which accounts for model prediction uncertainty is shown clearly in a hypothetical example shown in Figure 1 where the hypothetical response variable is product concentration. In this example the Hunter Reiner method will design an optimal experiment at a control variable value of 4. However, this experimental design, despite maximising the divergence between model predictions is actually a poor design as the model prediction uncertainty zones are overlapping. Instead the optimal design should be at control variable equal to 0, where the divergence between models is smaller, but the model uncertainty is also smaller and is not overlapping.

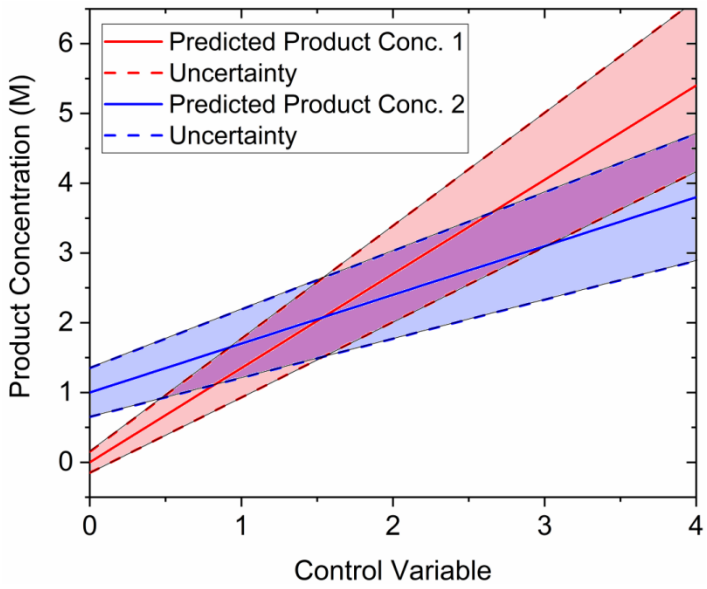

Figure 1. Example demonstrating model discrimination, based on example first shown by Box and Hill[42].

2.1.5 Model-Based Design of Experiments for Parameter Precision

MBDoE can be used to design experiments in order to give the most precise parameter estimates for a given model. This is done by calculating the value of the expected covariance matrix $\widehat{\mathbf{V}}_\theta$, after N_d new experiments are conducted, by using the additivity of Fisher information, as shown in Eq 14. Here, $\mathbf{V}_{\theta,0}$ refers to the a-priori covariance matrix, as calculated from the already completed N_{exp} experiments, while $\widehat{\mathbf{H}}_\mathbf{i}$ is the expected Fisher information to be collected from N_d new experiments[3, 48]. The expected information matrix for each designed experiment is calculated using the current parameter estimate $\widehat{\boldsymbol{\theta}}$.

$$\widehat{\mathbf{V}}_\theta(\widehat{\boldsymbol{\theta}}, \boldsymbol{\varphi}) = \left[\mathbf{V}_{\theta,0}^{-1} + \sum_{i=1}^{N_d} \widehat{\mathbf{H}}_\mathbf{i}(\widehat{\boldsymbol{\theta}}, \boldsymbol{\varphi})\right]^{-1} \tag{14}$$

The optimal experimental conditions can then be obtained by minimising a measure of the expected covariance matrix. For the minimisation, some scalar quantity is required to describe the covariance matrix. In this work the D-optimal criterion is used, where the determinant of the predicted covariance matrix was minimised. However, other popular criteria include A- and E-optimal which respectively minimise the trace and largest eigenvalue of the predicted covariance matrix[3, 48].

2.1.6 Practical Identifiability for a Given Experimental Budget

Model identifiability refers to if a model's parameters can be uniquely estimated, and this depends on the model structure and the experimental data available. Identifiability analysis, which has been reviewed by Miao et al[49], can be broadly divided into structural and practical identifiability. Structural identifiability analysis can be conducted by examining the model's equations and this is unaffected by the quality of the experimental data, whereas practical identifiability, which is the focus of this work, examines if a model's parameters are identifiable with a given experimental data set. Generally as the number of parameters in a model increase, it gains improved data fitting capabilities at the cost of the parameters being increasingly difficult to estimate (reduced identifiability). For a structurally identifiable model, practical identifiability is normally improved as more experiments are conducted.

There are many different ways to study identifiability, Marquardt et al have used linear algebra methods to check if unique solutions to model equations exist[50] and also by examining the Fisher Information Matrix, as identifiability is lost if its determinant approaches zero[51]. However, in this work practical identifiability is assessed for a given experimental budget by simulating the campaign of experiments, conducting parameter estimation with the simulated data set and checking if the predicted t-values exceed the reference t-value. The proposed procedure for testing a model's practical identifiability for a given experimental budget is shown in a flowchart in Figure 2. The first step is to quantify the capabilities of the available experimental set-up; this includes determining the allowable design space for the control variables and defining the measurement error for all measured model responses. Secondly the maximum number of experiments to be conducted is chosen; this is known as the experimental budget and is based on the time and cost to be dedicated to the project. Then the experimental campaign can be designed, which is an important step as the experimental design influences how much information is obtained from the campaign. While the most rigorous method to design the campaign of experiments is to first design a small number of experiments by factorial or Latin square design, followed by sequential design of each experiment with MBDoE, this can be computationally expensive, especially if there is a large experimental budget, as this requires that the parameter estimation and MBDoE optimisation be repeated for each experiment. Therefore, it is more efficient to first test the model with a computationally cheap experimental design, such as spending the entire experimental budget on a single factorial or Latin square design. If this design leads to an unidentifiable model, the process can be repeated with the more thorough MBDoE method to identify if better experimental design can improve identifiability, hence saving computational resources for only when they are needed. The next step is to choose values for the model parameters for each candidate model, so that these parameters can later be used to simulate experiments. An educated guess for the values of the model parameters can be made from previously collected experimental data, from information available in the literature or from researcher experience. This is an important step as the value of the parameters can influence practical identifiability. Therefore, if there is very little prior information to estimate parameter values, the model identifiability test can be repeated numerous times with different sets of parameters. Finally, with the chosen experimental design and parameter estimates, the campaign of experiments should be simulated, with the

appropriate level of measurement noise. The data obtained from this simulated campaign is then used for parameter estimation, and t-values are calculated for each model parameter. If the t-values for all parameters are greater than the reference t-value at 95% confidence level and for the given degrees of freedom, the model is declared practically identifiable. However, if any one of the parameter t-values fails the t-test, the model is declared practically unidentifiable for that experimental data set. For practically unidentifiable models the practical identifiability test can be repeated with improved experimental designs, through the use of MBDoE, however if it continues to fail the t-test the model is considered to be practically unidentifiable for the given experimental set-up and experimental budget.

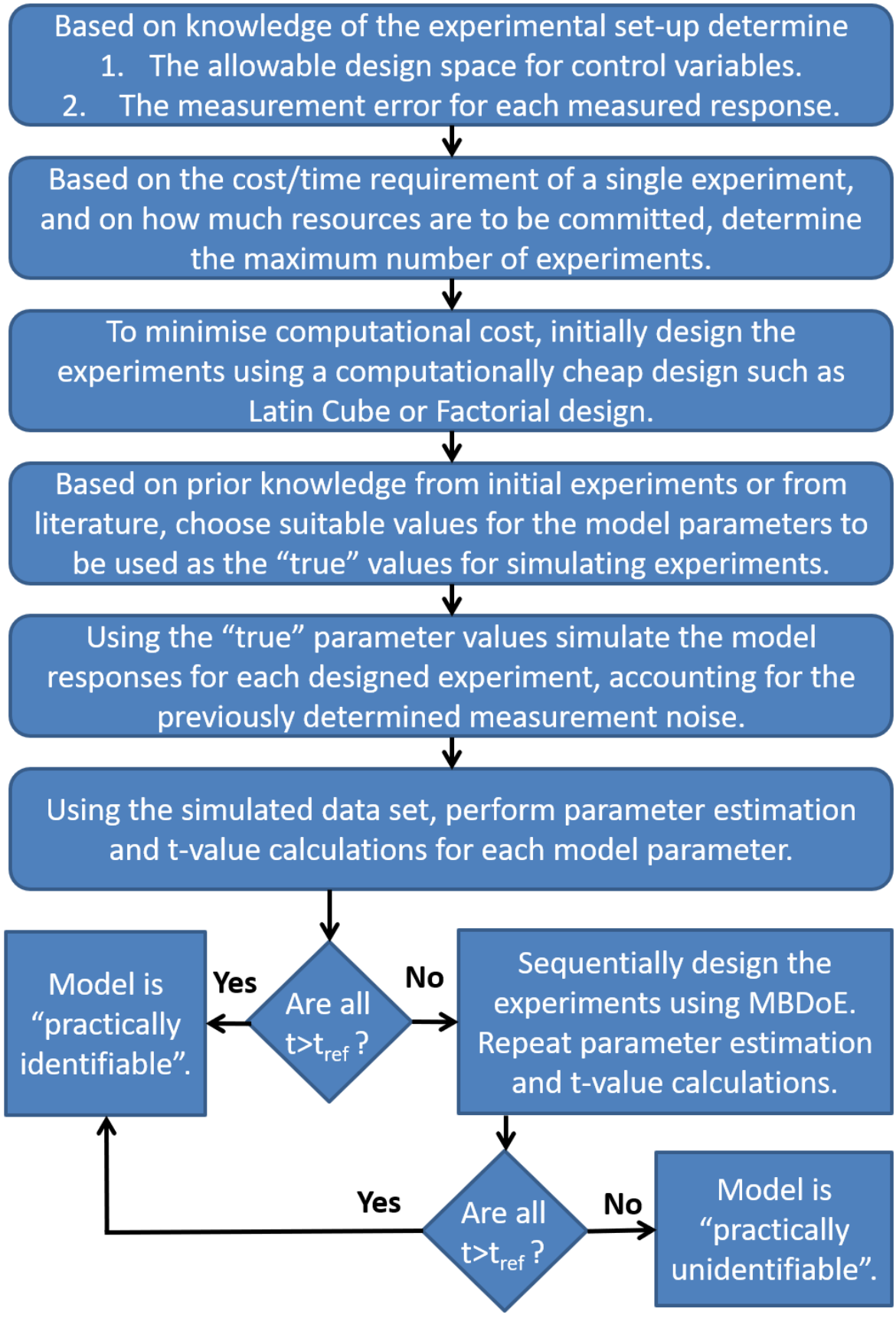

Figure 2. Flow chart demonstrating the steps in testing the practical identifiability of a single candidate model for a given experimental budget. This procedure should be repeated for each of the other candidate models.

2.2 Reaction & Candidate Kinetic Models

The esterification of benzoic acid and ethanol using the solid acid catalyst Amberlyst-15 (Sigma-Aldrich), shown in Eq 15, was chosen as the case study for this work, because Amberlyst-15 is known to be quite stable preventing any possible problems with deactivation and because there are no undesired side reactions.

$$Benzoic\ Acid + Ethanol \rightleftarrows Ethyl\ Benzoate + Water \tag{15}$$

Amberlyst-15 is a sulfonic acid, macroreticular polymeric resin based on crosslinked styrene divinylbenzene copolymers. The catalyst particles are spherical with particle diameters ranging from 0.35 mm to 1.18 mm. Each catalyst sphere is composed of a porous network of agglomerates of randomly packed gel microspheres, which gives the catalyst a high surface area and porosity[52, 53].

Based on kinetic studies in the literature for similar esterification reactions[54, 55], a number of candidate kinetic models are assumed for this reaction, including simple power law models (M1) and Langmuir Hinshelwood models at various levels of complexity (M2, M3 and M4). Due to the large excess of ethanol used (molar ratio greater than 9:1), the reverse reaction is considered to be negligible[56].

$$r'_{BA} = -kC_{BA}C_{EtOH} \tag{M1}$$

$$r'_{BA} = \frac{-kC_{BA}C_{EtOH}}{(1 + K_W C_W)^2} \tag{M2}$$

$$r'_{BA} = \frac{-kC_{BA}C_{EtOH}}{(1 + K_W C_W + K_{EtOH}C_{EtOH})^2} \tag{M3}$$

$$r'_{BA} = \frac{-kC_{BA}C_{EtOH}}{(1 + K_{BA}C_{BA} + K_{EtOH}C_{EtOH} + K_W C_W + K_{EB}C_{EB})^2} \tag{M4}$$

In these kinetic models the terms K_{BA}, K_{EtOH}, K_W and K_{EB} are the adsorption terms for each species, which are parameters to be estimated. In all cases the rate constant, *k*, is expressed in the re-parameterised Arrhenius form with two parameters *KP1* and *KP2* as shown in Eq 16, as this dramatically reduces correlation between the pre-exponential factor and the activation energy[57]. Here, T is temperature (K), and T_M is the mean temperature of 378.15 K, calculated as the average value of the upper and lower temperature limits for this experiment.

$$k = exp\left(-KP1 - \frac{KP2 * 10000}{R} * \left[\frac{1}{T} - \frac{1}{T_M}\right]\right) \tag{16}$$

The original Arrhenius parameters k_0 and *Ea* can be obtained from the re-parameterised parameters *KP1* and *KP2* according to

$$k_0 = exp\left(-KP1 + \frac{KP2 * 10000}{R * T_M}\right) \tag{17}$$

$$E_a = KP2 * 10000 \tag{18}$$

When proposing simplified versions of the Langmuir Hinshelwood model (M2 and M3), the adsorption terms for benzoic acid and ethyl benzoate were the first to be neglected as the literature reports that the these adsorption terms are less significant than the more polar water and ethanol species[54, 55]. When developing a further simplified Langmuir Hinshelwood (M2) model the ethanol adsorption term was also removed from the model, because as the concentration of ethanol was in excess, it would be approximately constant.

2.3 Experimental Set-up

A bead string reactor, where the reactor internal diameter is only slightly larger than the catalyst particle as shown in Figure 3, was chosen for this reaction. A picture of the bead string reactor is also shown in the SI. String reactors (bead strings or pellet strings etc.) i) provide plug flow behaviour with negligible bypass or axial dispersion[58], ii) possess efficient heat transfer due to the large surface area to volume ratio[58], iii) allow the use of similar superficial velocities to those that are used in industrial scale reactors[58-61] iv) increased reproducibility between reactors as packing is always uniform[58, 59] v) ease of scale-up through parallelisation[62] and vi) they use industrial sized catalyst pellets instead of smaller particles or powders, hence allowing the study of any catalyst pellet skin effects[63]. The bead string reactor consisted of a PTFE tubing (VICI Jour) with external diameter of 1.58 mm and internal diameter of 1 mm, into which Amberlyst-15 spheres obtained from the 710-850 µm dry sieve fraction were loaded, which due to the swelling of Amberlyst, resulted in an average wet diameter of 825 µm as measured by a microscope (VHX-600 Digital Microscope, Keyence), and hence giving a reactor aspect ratio (reactor diameter divided by catalyst diameter) of 1.2. A typical reactor was loaded with 0.1 g of Amberlyst-15 resulting in a catalyst bed length of 30 cm. In order to hold the catalyst in place a nickel mesh (Tecan, UK) of 25 µm thickness and 25 µm hole diameter was placed at the reactor outlet by compressive force between a PEEK union (Upchurch) and a PEEK ferrule (Upchurch).

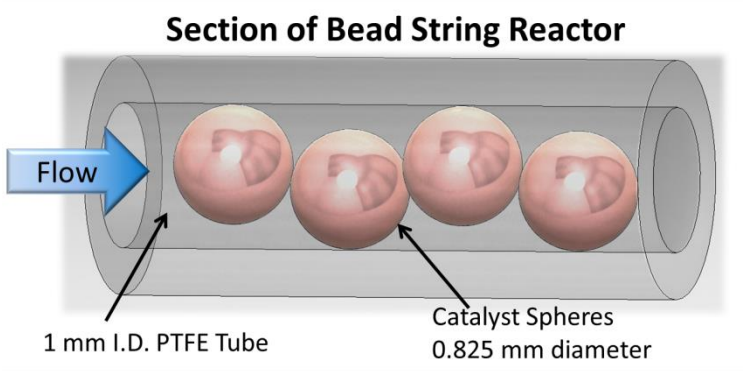

Figure 3. A section of the bead string reactor showing the PTFE tubing with 1.58 mm outer diameter and 1 mm inner diameter, filled with 0.825 mm diameter Amberlyst-15 spheres.

In order to confirm that the reactor behaved as a plug flow reactor, a step change Residence Time Distribution (RTD) study was conducted at four different flowrates in the area of interest for the kinetic study, (10, 20, 40 and 80 µL/min). This RTD study is shown in the Supporting Information, and confirmed that the reactor could be reasonably modelled as a plug flow reactor as the vessel dispersion numbers ranged from 0.01-0.02. Additionally, an external mass transfer study was conducted using the copper dissolution method[64] to demonstrate that external mass transfer resistances could be neglected for this reaction, full details are shown in the Supporting Information. The internal mass transfer resistances were assessed using the Weisz-Prater criterion, which showed that there were no mass transfer resistances inside the Amberlyst-15 particles (full details are shown in the Supporting Information). However, Amberlyst-15 has a macro-reticular structure where each catalyst particle is composed of smaller microspheres, and in the literature there is evidence to suggest that there are internal mass transfer resistances inside these microspheres that can only be observed if the catalyst is ground to break the smaller microspheres[65]. As this mass transfer resistance inside the microspheres is not accounted for, the models developed in this work can be considered as

apparent kinetic models. However, these models are still applicable for reactor design, as long as the catalyst particles are not ground into a powder.

Having confirmed that the reactor had approximately plug flow behaviour and that is was reasonable to neglect external mass transfer, the reactor was then modelled using the steady-state ideal plug flow equation as shown in Eq 19, where W is the catalyst mass (g), r'_{BA} is the rate of reaction of benzoic acid (mol g^{-1} s^{-1}) and v is the inlet liquid flowrate (L/s).

$$\frac{dC_{BA}}{dW} = \frac{r'_{BA}}{v} \tag{19}$$

The kinetic experiments were conducted by a closed-loop autonomous reactor platform shown in Figure 4, which was previously used with a flow microreactor for the homogenous esterification of benzoic acid with sulfuric acid catalyst [40]. The experimental set-up consisted of four 5 mL glass syringes (Cetoni) being driven by a syringe pump (neMESYS low pressure module, Cetoni) where two syringes were filled with a low concentration benzoic acid in ethanol solution (0.85 M) and the other two syringes were filled with high concentration benzoic acid in ethanol (1.65 M). Each pair of syringes was connected by a T-junction (UpChurch) and the fluids were mixed at a Y-junction (UpChurch) before entering the string reactor. By varying the flowrate ratio of the two syringes it was possible to obtain any feed concentration desired between the concentrations in the two syringes. Four syringes were used instead of just two to increase the volume of reagents available for experiments before the syringes emptied requiring the experiment to end. The maximum flowrate allowed was set at 60 µL/min to prevent the syringes emptying too quickly and a minimum flowrate of 15 µL/min was chosen to keep the residence time small enough that an experiment could be completed in a reasonable amount of time. The string reactor was submerged in an oil bath which was heated by a loop cartridge heater (OMEGALUX FGR 6 foot length, 250 W); the maximum allowable temperature was 120 °C, as that is the maximum operating temperature of Amberlyst-15. In order to ensure that the reactants reached the reaction temperature before they reached the packed Amberlyst section of the string reactor, a section of 7 cm of the tubing was filled with inert glass beads (425-600 µm, Sigma Aldrich) upstream of the Amberlyst-15 packed section to act as a preheating section (see the Supporting Information for more details). The reactor outlet was connected to the 6-way switching valve of a sampler-dilutor (Syrris Asia) to allow online analysis by HPLC before flowing into a pressure vessel. The pressure vessel consisted of a 50 mL centrifuge tube with a custom made PEEK top with three inlet connections designed to withstand high pressures. In order to prevent evaporation of the ethanol solvent, the entire system was pressurised to 6 barg with nitrogen using a mass flow controller (SLA mass flow controller, Brooks) and a back-pressure regulator (Swagelok K series, 250 psig). There was a liquid pressure sensor (Zaiput, Hastelloy 300 psi, ~10 µL dead volume) placed before the reactor

entrance to measure the pressure drop in the reactor and a gas pressure sensor (Honeywell 40PC 250 psig) connected to the pressure vessel.

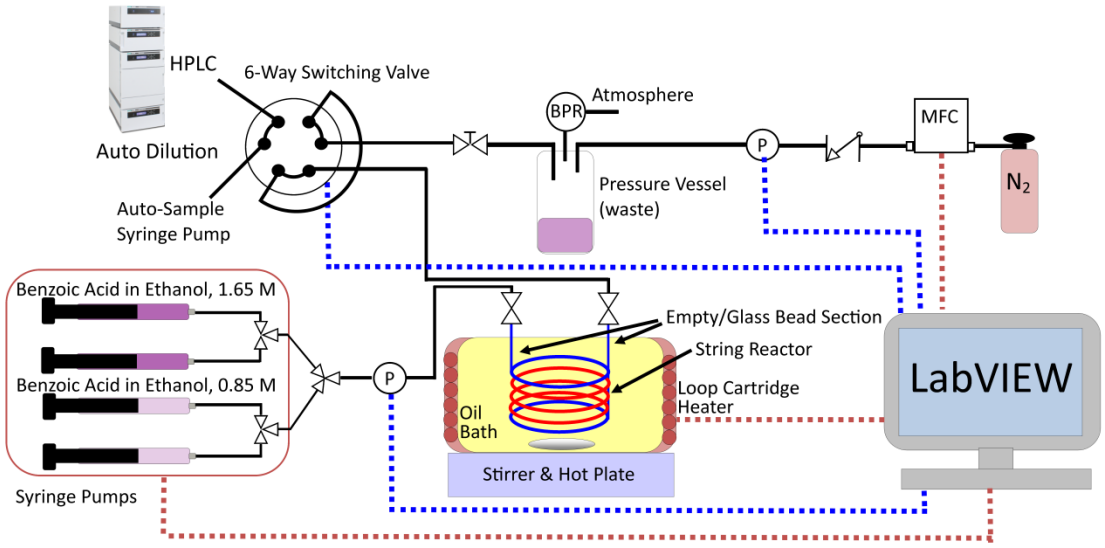

Figure 4. Autonomous reactor platform used for the kinetic experiments for the esterification of benzoic acid and ethanol using Amberlyst-15 as a heterogeneous catalyst in a string reactor. Red dashed lines indicate LabVIEW controls the equipment, blue dashed lines indicate LabVIEW reads the measurement from the equipment. BPR, MFC and P indicate back-pressure regulator, mass flow controller and pressure sensor, respectively.

The outlet concentration of benzoic acid and ethyl benzoate was measured by online HPLC (Jasco LC-4000) using a 250 mm long, 4.6 mm i.d. ODS hypersil column with 5 µm particle size (Thermo Fisher Scientific). The HPLC analysis duration was less than 7 min with a flowrate of 1.25 mL/min of 60:40 acetonitrile: DI water. The column oven was maintained at 30 °C and the detection was achieved using a UV-vis detector at 274 nm. The sampler-dilutor applied a dilution factor of 250 using a mixing chip (Micromixer Chip, Dolomite) before injecting a sample to the column. The measurement error was determined from replicated experiments, and a constant error model was used with a standard deviation of 0.030 M and 0.0165 M for benzoic acid and ethyl benzoate respectively. This error was due to the combined error in the measurement system (there was a large dilution factor) and the experimental control (accuracy of the syringe flowrates, etc.).

The experimental system was monitored and controlled by LabVIEW, which controlled temperature, feed concentration and liquid flowrate as well as measured the temperature, pressures and the outlet concentrations of benzoic acid and ethyl benzoate. The LabVIEW code was used to automatically run a campaign of steady-state experiments, which were either chosen in advance by the user, or designed automatically using MBDoE methods. Python was integrated in the LabVIEW code to perform online parameter estimation and MBDoE. Online parameter estimation was achieved using the Nelder-Mead simplex algorithm[66], and the initial parameter guess required for this algorithm was based on the results of initial experimental data. Online MBDoE for both model discrimination and improved parameter precision was performed using the SLSQP (Sequential Least Squares Programming) algorithm which requires an initial guess for the design vector. In order to prevent the algorithm being stuck in a local optimum, 10,000 guesses for the design vector were generated and simulated, the best design vector of these 10,000 screening guesses was determined based on the objective criteria (either Eq 10 or Eq 14) and this best design was used as the initial guess for the SLSQP optimiser. This screening procedure was performed online every time MBDoE was performed. Additionally, the

LabVIEW code included safety shutdown features, where if the temperature or pressure exceeded a certain value or if a syringe emptied, the heaters and syringe pumps would be automatically turned off. The various pieces of lab equipment were integrated with LabVIEW through the use of equipment drivers. Since there was no driver available for the HPLC system (Jasco), the HPLC was set, using the Jasco ChormeNav software, to automatically sample the reactor outlet every 7 min and to send the results to an Excel file. As LabVIEW is able to access and read Excel files, this allowed the simple integration of a complicated piece of equipment with LabVIEW[14].

2.4 Experimental Design Procedure

In all kinetic studies, the quality of the models developed in terms of both identifying an appropriate model structure and obtaining precise parameter estimates is controlled by the size of the experimental design space, the magnitude of the experimental error and the number of experiments allowed in the experimental budget. However, through the use of the methodology described in the following section and shown in Figure 5, it is possible to get the most out of the available experimental set-up in terms of minimising the number of experiments required for kinetic model identification. This is a general methodology that can be applied to any kinetic study and not just to this case study.

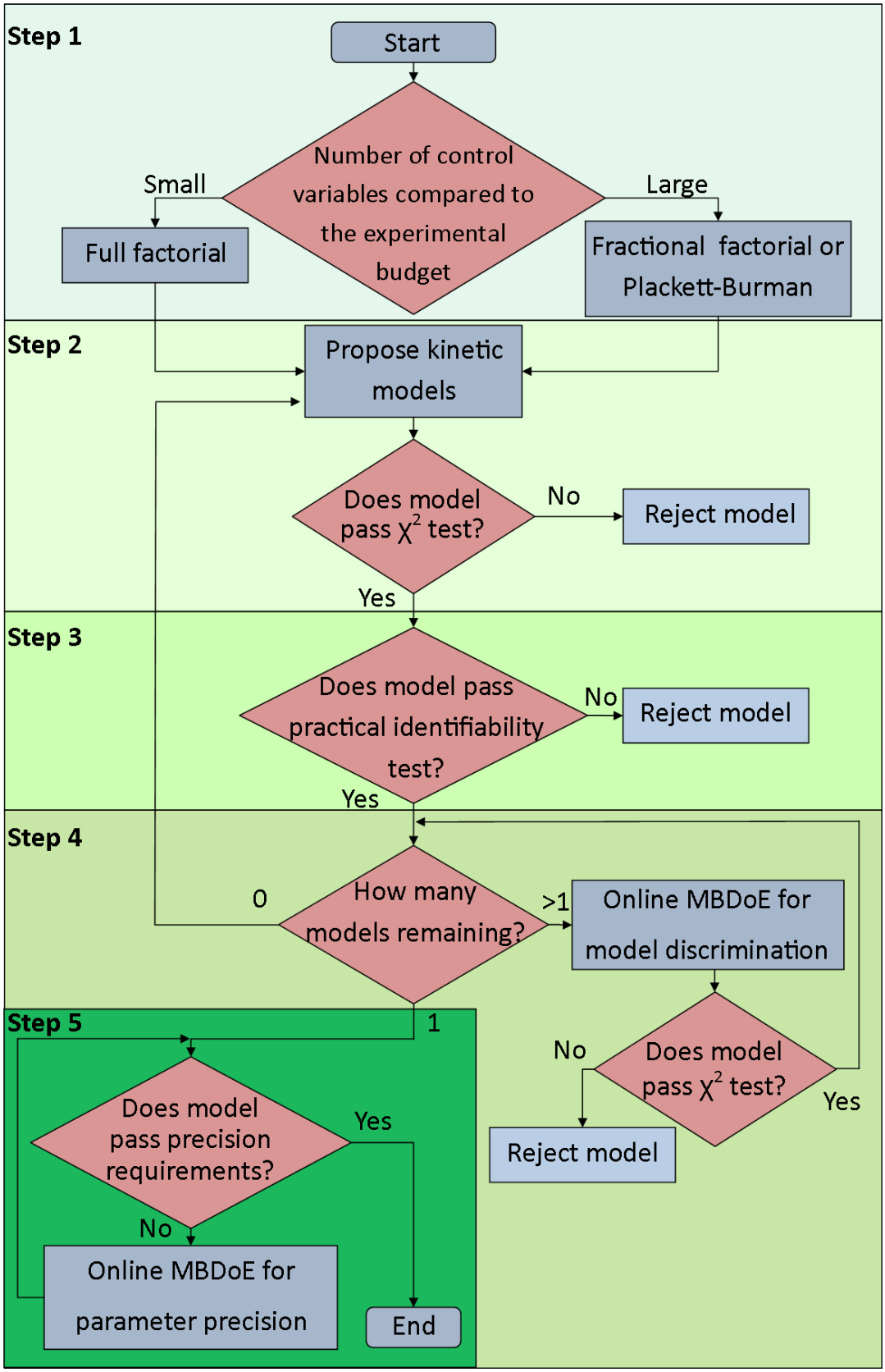

Figure 5. Flowchart showing the experimental methodology that can be applied to any general kinetic study.

Step 1. Factorial Screening & Catalyst Stability Check. In some cases if there is prior information available from the literature, it may be most efficient to immediately begin with MBDoE experiments

designed for improved parameter precision and then continue on to step 2. However, if there is no prior information about the reaction (which is assumed to be the case for this work), then the best start is to perform a traditional design of experiments[67]. In this case, where there are only three control variables (temperature, flowrate and feed concentration), it is reasonable to carry out a full factorial design at two levels, consisting of 8 steady-state experiments. Here, the levels for each variable were 100 °C and 120 °C, 20 µL/min and 40 µL/min and 1 M and 1.5 M benzoic acid feed concentration. However, in more general cases, if there were a larger number of control variables a fractional factorial or Plackett-Burman design could be used[67]. In addition to the factorial screening, in order to check the stability of the catalyst, the 1st experiment conducted every day was repeated at the end of the day. Furthermore a new reactor was packed at the beginning of every day.

Step 2. Propose and Test Candidate Rate Laws. Candidate kinetic models can be proposed and tested against the initial experimental data collected from the factorial campaign, they can be chosen from the literature or suggested by the user. Any candidate model that fails the 95% χ^2 test, as calculated from Eq 4, or has a parameter estimate whose entire 95% confidence interval is not realistic (e.g. negative activation energies), is rejected. All other models proceed to the next step.

Step 3. Practical Model Identifiability for a Given Experimental Budget. In order to reject models which are practically unidentifiable for the available experimental set-up and experimental budget, an identifiability analysis is conducted, following the general procedure described in the previous section. In this case, the allowable design space is defined as 80–120 °C, 15–60 µL/min and 0.9-1.55 M, and then the maximum experimental budget is set at 64 experiments. The parameter values used to simulate the experiments are the maximum likelihood estimates obtained from performing parameter estimation with the experimental data from step 1, factorial screening. Normally distributed noise with standard deviations equal to the level expected in the real experimental set-up is added to all simulated experiments.

Step 4. Online MBDoE for Model Discrimination. In order to identify the correct model from all the other candidate models that both fit the preliminary data and pass the practical model identifiability test, experiments should be conducted using online MBDoE for model discrimination with the Buzzi-Ferraris criterion[43, 44]. Multiple experiments are conducted until all but one model is rejected for failing the 95% χ^2 test. If it is not possible to distinguish between two or more models after a large number of discriminating experiments, it may be because the model uncertainty is too large and hence experiments have very little discriminating power. In this case it may be more useful to conduct a small number of experiments targeted at improved parameter precision for one of the candidate models, so that the model uncertainties can be reduced, hence making discrimination easier. If this does not work, the models may be too similar to distinguish for the given design space and the given level of experimental error. In this case, one of the models is chosen and brought forward to step 5. Alternatively, if all models fail the χ^2 test it may be necessary to develop new models. It may be the case that all of the suitable models are rejected in the practical identifiability test. If this is the case, it is suggested to increase the maximum experimental budget to try and assist more models getting through the practical identifiability test.

Step 5. Online MBDoE for Improved Parameter Precision. With the single chosen model, experiments are now designed using online MBDoE for improved parameter precision (see Eq 14), until a desired level of parameter precision is achieved, at which point the model is considered identified.

Note that the experimental system is capable of automatically performing all of the experimental steps in this methodology, steps 1, 4 and 5. However, the system does not automatically switch from one step to another. In the case of the factorial experiments in step 1, the platform will automatically stop once the final pre-defined experiment is finished, but for steps 4 and 5 where experiments are designed online by MBDoE, the system will run an infinite number of experiments unless the user intervenes and stops the experiments. Therefore, the user must manually select when to swap from discriminating experiments to parameter precision experiments. This decision is aided by the parameter statistics displayed on the LabVIEW user interface, which are automatically updated with each successive experiment.

3. Results & Discussion

Step 1. Factorial Screening & Catalyst Stability Check. The first kinetic experiments conducted were a campaign of 8 experiments designed by the factorial method. The experimental conditions are shown in Figure 6a, while the outlet concentrations are shown in Figure 6b, and are also reported in the Supporting Information. In order to assess the stability of the catalyst, after the 8 experiments were completed, a 9th experiment was run at the same conditions as the first experiment. As shown in Figure 6b, the outlet concentration of the first and ninth experiment are approximately the same indicating that the catalyst is stable and no deactivation is present.

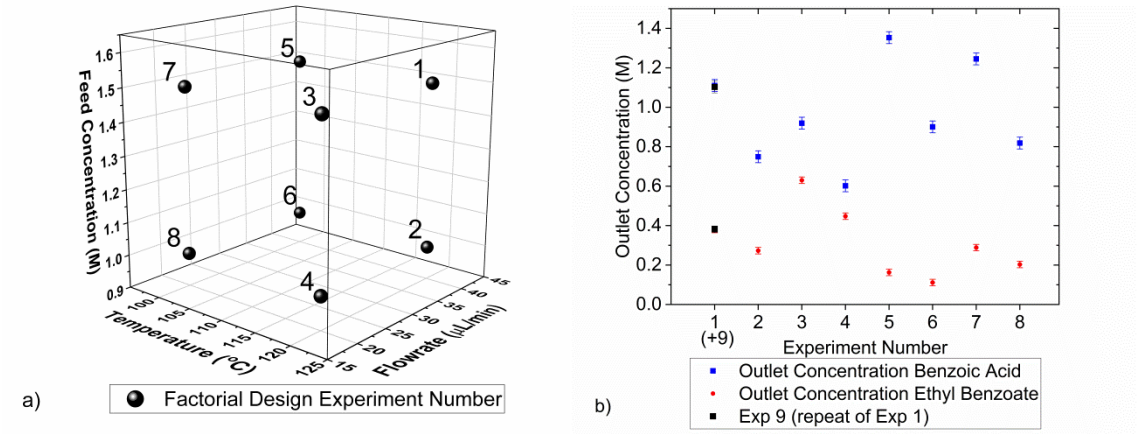

Figure 6. a) The experimental conditions of the 8 steady-state experiments designed by the factorial method. b) The outlet concentrations measured from these experiments.

Step 2. Propose and Test Candidate Rate Laws. Using the data set obtained from the 8 factorial experiments, parameter estimates and 95% χ^2 tests are calculated for each candidate model. It was found that all 4 models passed the 95% χ^2 test after the initial 8 experiments and therefore all models are brought forward to step 3. The parameter estimates, 95% confidence intervals and χ^2 values for each candidate model are reported in the Supporting Information.

Step 3. Practical Model Identifiability for a Given Experimental Budget. The experimental conditions designed from the four level factorial design are shown in Figure 7. The results of these simulated experiments show that model M3 and M4, which are Langmuir Hinshelwood type models with 4 and 6 parameters, are practically unidentifiable for a campaign of 64 factorial designed experiments, as the predicted t-values for the adsorption parameters are below the t-reference value, as shown in

Table 1. Further parameter statistics including the parameter estimates and 95% confidence interval values are reported in the Supporting Information.

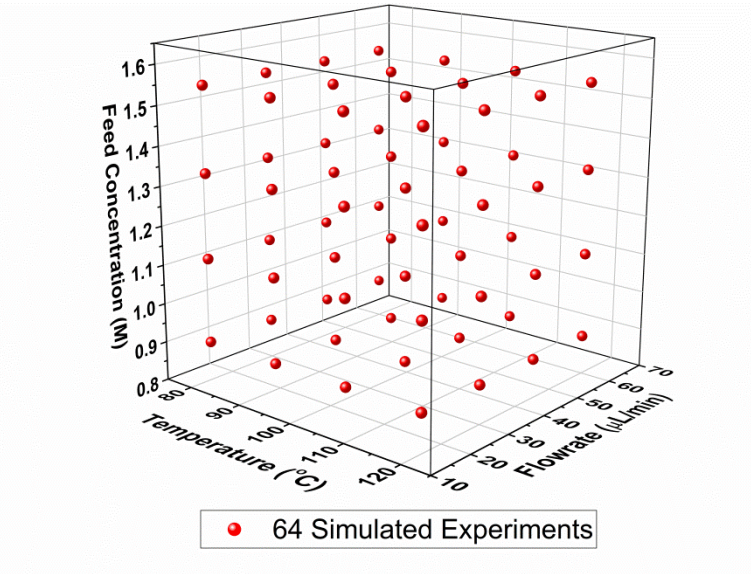

Figure 7. Experimental conditions for the simulated experiments for the practical model identifiability test in Step 3, designed by the factorial method.

Table 1. The predicted t-values for the parameters in each model estimated after parameter estimation with the data set obtained from the simulated campaign of 64 experiments designed by a four-level factorial campaign.

	Reaction Rate Law	Predicted t-values (reference = 1.657)						Action
		KP1	*KP2*	K_W	K_{EtOH}	K_{BA}	K_{EB}	
M1	$kC_{BA}C_{EtOH}$	681	26.6	/	/	/	/	Accept
M2	$\frac{kC_{BA}C_{EB}}{(1+K_WC_W)^2}$	326	22.0	1.95	/	/	/	Accept
M3	$\frac{kC_{BA}C_{EB}}{(1+K_WC_W+K_{EtOH}C_{EtOH})^2}$	8.83	21.4	**0.63**	**0.34**	/	/	**Reject**
M4	$\frac{kC_{BA}C_{EB}}{(1+K_{BA}C_{BA}+K_{EtOH}C_{EtOH}+K_WC_W+K_{EB}C_E}$	**0.87**	19.6	**0.02**	**0.10**	**0.10**	**-0.01**	**Reject**

For model M3, which failed the factorial designed practical identifiability test, the practical identifiability was then repeated using MBDoE to improve the predicted t-values, of the 64 simulated experiments, the first 8 were designed using a factorial method and the remaining 56 were designed using sequential MBDoE. This was not done for model M4 as model M4 was not even close to being practically identifiable for this experimental budget and design space. Due to the introduction of random noise in the simulated experiments, the results of these practical identifiability tests vary each time the simulation is performed, therefore this procedure was conducted twice using D-optimal MBDoE and twice using E-optimal MBDoE. The designed experiments are shown in Figure 8 and the predicted t-values for these simulated MBDoE campaigns are reported in the Supporting Information. The results show that the predicted t-values for both K_W and K_{EtOH} improve, however, they do not increase enough to pass the t-test. Therefore, both model M3 and M4 were rejected due to them being practically unidentifiable and only models M1 and M2 were brought forward to step 4. This is

not an unusual result, as the estimation of all of the adsorption terms in the Langmuir Hinshelwood equation is frequently so difficult that the use of simplified Langmuir Hinshelwood rate laws is common in the literature[54]. Furthermore in the cases where studies report kinetic parameters for the full Langmuir-Hinshelwood rate law, they usually just report parameter values without confidence intervals or t-values[55], therefore it is possible that these estimated values are actually estimated poorly with large confidence intervals.

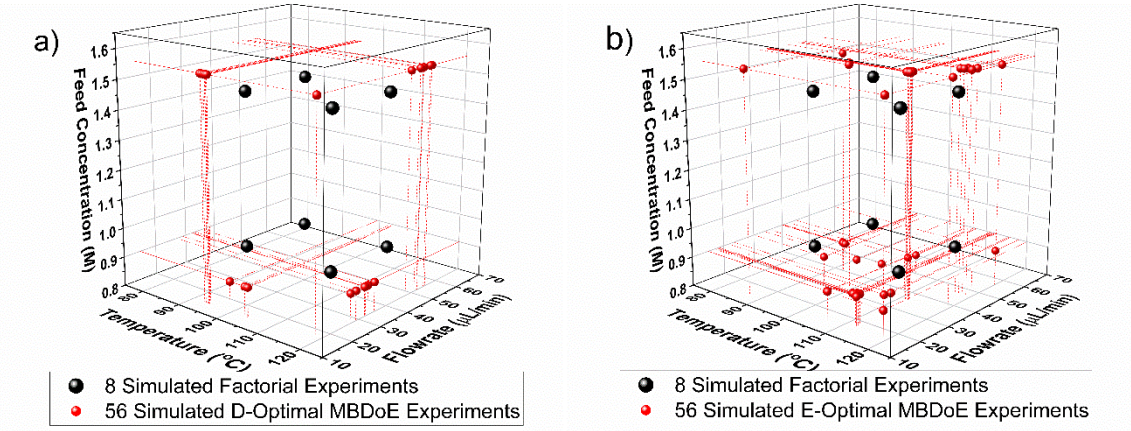

Figure 8. Experimental conditions of the 64 simulated experiments sequentially designed by a) D-optimal MBDoE and b) E-optimal MBDoE, for testing practical identifiability of model M3.

The practical identifiability step is important as time is not wasted pursuing models that are not identifiable with the available experimental set-up and experimental budget. Therefore, rather than pursuing a model which may be the true mechanistic model, such as the 6 parameter Langmuir Hinshelwood model M4, instead resources are better spent obtaining a practical model such as the simplified 3 parameter Langmuir Hinshelwood model M2, that can describe the reaction behaviour in the allowable design space. While it can be argued that simplified models will behave poorly when extrapolated outside of the design space they were developed in, this is also the case for true models if their parameters are estimated poorly. Furthermore, while simplified model structures give less mechanistic information about the behaviour of the catalyst, they can still be used for reactor design and process control, as long as the process conditions are within the domain of model validity. Therefore, in many industrial applications a simplified model could be sufficient.

Step 4. Online MBDoE for Model Discrimination. The number of candidate models is now reduced to 2 after models M3 and M4 were rejected for being practically non identifiable for this experimental set-up and budget. In order to distinguish between the remaining two models, model M1 and model M2, a campaign of online experiments designed by the Buzzi-Ferraris method of MBDoE for model discrimination[43, 44] was conducted using the autonomous reactor platform. The initial 8 experiments from the factorial campaign were used as preliminary information when designing discriminating experiments. The designed experimental conditions are shown in Figure 9, and they are reported along with the measured outlet concentrations in the Supporting Information. The statistics after each experiment are shown in Table 2, where it can be seen that model M1 can be rejected after just 1 discriminating experiment as it failed the 95% χ^2 test. However, the automated system did not have a stop condition to automatically detect when to stop performing model discrimination and when to perform MBDoE for parameter precision. Therefore three more experiments for model discrimination

were designed online and executed before the user intervened and changed the design criteria to MBDoE for parameter precision with model M2.

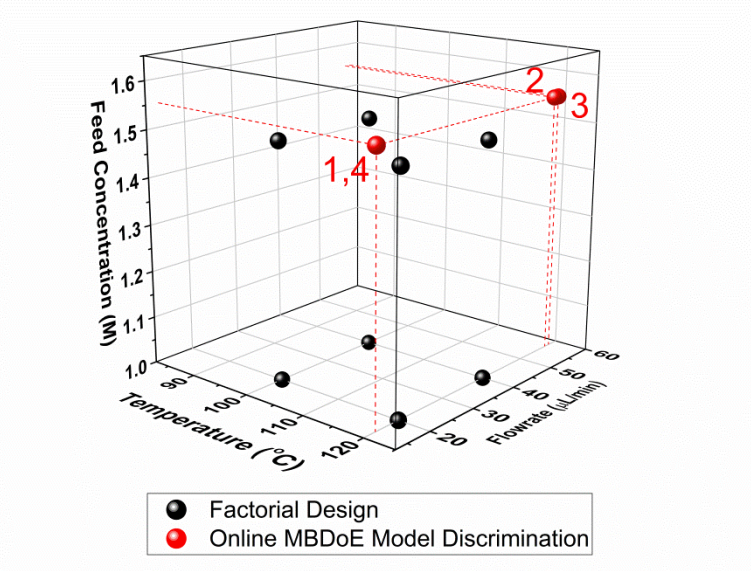

Figure 9. Experimental conditions of the MBDOE-designed discriminating experiments during Step 4. Numbers indicate the order in which experiments were designed and conducted.

Table 2. The χ^2 values obtained by online parameter estimation conducted after each successive model discrimination experiment designed online by MBDoE as part of Step 4. In the "Experiments Conducted" column, MD1 to MD4 refer to the four experiments designed by online model discrimination.

Experiments Conducted	Model M1 χ^2/χ^2ref	Model M2 χ^2/χ^2ref	Action
8 Factorial	10.5/23.7	7.34/22.4	Accept Both Models
8 Factorial + MD1	**35.4/26.3**	13.5/25.0	**Reject Model 1**
8 Factorial + MD2	**37.6/28.9**	17.9/27.6	**Reject Model 1**
8 Factorial + MD3	**41.9/31.4**	24.2/30.1	**Reject Model 1**
8 Factorial + MD4	**54.7/33.9**	26.9/32.7	**Reject Model 1**

Interestingly, by examining how the parameter statistics change with each successive experiment for the accepted model structure M2 (which are reported in the Supporting Information), it is observed that after the 4th discriminating experiment, that all the parameters in model M2 passed the t-test. This is significant as passing the t-test for all parameters is frequently used as the criterion for identifying a model and ending the experiments.

Step 5. Online MBDoE for Improved Parameter Precision. The single candidate model, M2, which is both practically identifiable and capable of fitting all the experimental data collected, was already identified in the model discrimination stage, as all the parameters passed the t-test. However, in order to improve the confidence in which the parameters are known, and to hence improve model prediction certainty, a campaign of online MBDoE experiments for improved parameter precision using the D-optimal criterion was performed by the autonomous reactor platform. The experimental measurements from the 8 factorial experiments and the 4 discriminating experiments were provided to the MBDoE algorithm to give prior information about the system. The experimental conditions designed by the MBDoE algorithm are shown in Figure 10, and are reported in the Supporting Information, (along with the measured outlet concentrations and detailed parameter statistics). The automated system was stopped by user intervention at the end of a working day, when it had already

designed and preformed 8 experiments. The parameter statistics after these 8 experiments, were found to have improved significantly compared to their values at the end of the model discriminating experiments, with the confidence intervals for parameters *KP1*, *KP2* and K_W being reduced from 0.11, 0.74 and 0.25 to 0.08, 0.45 and 0.2. At this point, the model is declared to be well identified with acceptable confidence intervals and no further experiments were considered necessary.

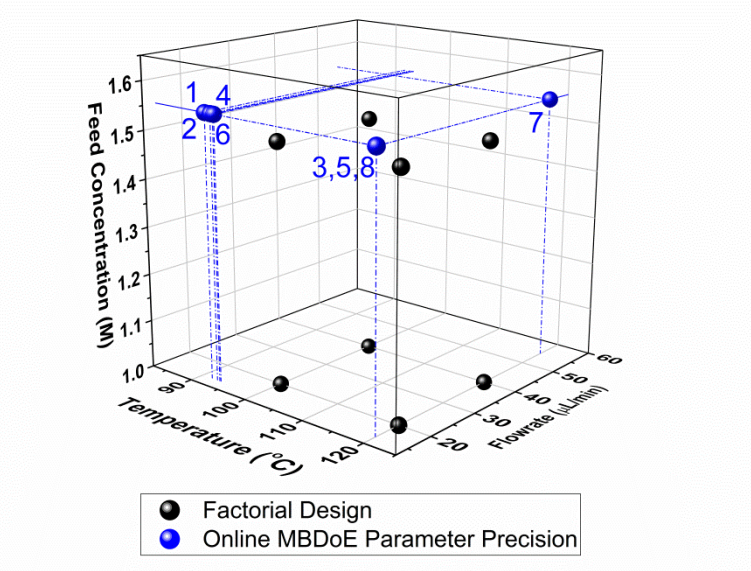

Figure 10. Experimental conditions of the D-optimal MBDOE-designed experiments for improved parameter precision during Step 5. Numbers indicate the order in which experiments were designed and conducted.

The final parameter estimates for *KP1*, *KP2* and K_W are converted back to the original form of the Arrhenius equation and the final rate expression is shown in Eq 20 where the pre-exponential factor k_0 was 185.3 $L^2\ g^{-1}\ s^{-1}\ mol^{-1}$, the apparent activation energy *Ea* was 68.8 kJ/mol and the adsorption constant of water K_W was 0.53 L/mol. In comparison with the literature, Pipus et al, reported a similar activation energy of 69.1 ±0.5 kJ/mol[56]. Further comparisons of the model parameters cannot be made as Pipus et al used a different model structure, they reported that the reaction could be modelled as second-order with respect to benzoic acid without any adsorption terms. Other work using a slightly different catalyst, Amberlyst-39, reported that the reaction was best described by a Langmuir-Hinshelwood mechanism with an activation energy of 79.9 kJ/mol[55].

$$r'_{BA} = \frac{185.3 * \ exp\left(-\frac{68800}{RT}\right) * C_{BA}C_{EtOH}}{(1 + 0.53C_W)^2} \quad (20)$$

The adequacy of the model developed in this work is demonstrated by passing the 95% χ^2 test and the parity plot in Figure 11.

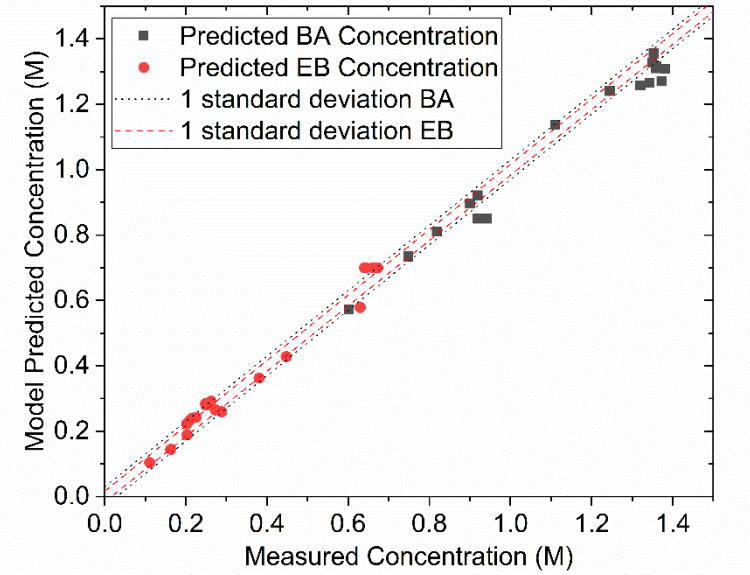

Figure 11. Parity plot for the model-predicted and experimentally measured concentrations of benzoic acid and ethyl benzoate.

It can be shown that the model prediction uncertainty decreased significantly after conducting the 8 MBDoE experiments for improved parameter precision, as shown in Figure 12 for one specific experimental condition (120 °C, 20 µL/min inlet flowrate, 1 M benzoic acid inlet concentration). This figure, showing the observed frequency of response values, is created using the multivariate normal distribution method previously described in the Parameter Precision section. Further model uncertainty graphs for other experimental conditions are shown in the Supporting Information. If even smaller confidence intervals were required it would be possible to continue performing further experiments designed by MBDoE, however the expected gain in information with further experiments is expected to be diminishing, unless changes to the experimental procedure allowed an exploration of a wider design space.

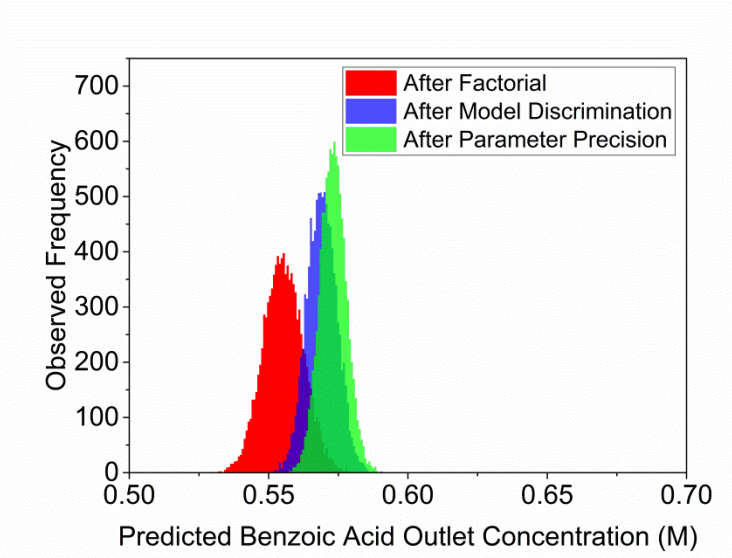

Figure 12. Model prediction for model M2 at a reaction temperature of 120 °C, an inlet flowrate of 20 µL/min and a feed concentration of 1.5 M benzoic acid and 0.1156 g of Amberlyst-15 catalyst after the factorial (Step 1), model discrimination (Step 4) and parameter precision campaigns (Step 5).

4. Conclusions

A bead string reactor was used for studying the kinetics of the esterification of benzoic acid and ethanol using the heterogeneous Amberlyst-15 catalyst, as it provided plug flow behaviour with efficient mass transfer to allow the study of the catalytic kinetics. Due to the macroreticular structure of Amberlyst-15 it was not possible to remove internal mass transfer resistances from the microspheres that make up the larger catalyst structure, and instead an apparent kinetic model is reported. The developed 5-step methodology offered a systematic way to identify practical kinetic models and in this case a simplified 3-parameter Langmuir Hinshelwood model was found to be the most appropriate kinetic model that combined practical identifiability, while also being able to describe the reaction in the experimental design space. The methodology proposed minimised the number of experiments required by preventing the pursuit of non-identifiable models, such as a 6-parameter Langmuir Hinshelwood model. Further reduction in the number of experiments was achieved by using online MBDoE for both model discrimination and for precise parameter estimation. A single MBDoE designed experiment for model discrimination was found sufficient to distinguish between two candidate models. The use of MBDoE for parameter precision gave the desired improvement in parameter precision, which then in turn reduced the uncertainty associated with model predictions. The use of a closed loop system in this work enabled the use of online MBDoE which was a key component of the experimental methodology and resulted in all of the kinetic experiments in this work being completed in just three days. Furthermore, the closed loop system also offered major time savings as it could be operated unsupervised, freeing up researcher time for other tasks.

Supporting Information

Images of the bead string reactor, details of the residence time distribution study, details of the external and internal mass transfer study, numerical values from the automated kinetic experiments

and their associated parameter statistics. This information is available free of charge via the Internet at http: //pubs.acs.org.

Acknowledgements

The authors CW and AP thank the department of Chemical Engineering in University College London for their PhD studentships, and MQ thanks the Hugh Walter Stern PhD Scholarship, University College London for his funding. All the authors express their gratitude to Dr Gaowei Wu who designed the custom made PEEK pressure vessel used in this work.

Conflicts of Interest

The authors have no conflicts of interest to declare.

References

(1) Hagen, J., *Industrial catalysis: A practical approach*. 3 ed.; John Wiley & Sons: Weinheim, 2015.
(2) Blackmond, D. G., Kinetic profiling of catalytic organic reactions as a mechanistic tool. *J. Am. Chem. Soc.* **2015,** *137*, 10852-10866.
(3) Franceschini, G.; Macchietto, S., Model-based design of experiments for parameter precision: State of the art. *Chem. Eng. Sci.* **2008,** *63*, 4846-4872.
(4) Blackmond, D. G., Reaction progress kinetic analysis: a powerful methodology for mechanistic studies of complex catalytic reactions. *Angew. Chem. Int. Edit.* **2005,** *44*, 4302-4320.
(5) Losey, M. W.; Schmidt, M. A.; Jensen, K. F., Microfabricated multiphase packed-bed reactors: Characterization of mass transfer and reactions. *Ind. Eng. Chem. Res.* **2001,** *40*, 2555-2562.
(6) Tadepalli, S.; Halder, R.; Lawal, A., Catalytic hydrogenation of o-nitroanisole in a microreactor: Reactor performance and kinetic studies. *Chem. Eng. Sci.* **2007,** *62*, 2663-2678.
(7) Hartman, R. L.; McMullen, J. P.; Jensen, K. F., Deciding whether to go with the flow: Evaluating the merits of flow reactors for synthesis. *Angew. Chem. Int. Ed. Engl.* **2011,** *50*, 7502-7519.
(8) Kockmann, N.; Thenee, P.; Fleischer-Trebes, C.; Laudadio, G.; Noël, T., Safety assessment in development and operation of modular continuous-flow processes. *Reac. Chem. Eng.* **2017,** *2*, 258-280.
(9) Patel, D. C.; Lyu, Y. F.; Gandarilla, J.; Doherty, S., Unattended reaction monitoring using an automated microfluidic sampler and on-line liquid chromatography. *Anal. Chim. Acta* **2018,** *1004*, 32-39.
(10) Malig, T. C.; Koenig, J. D. B.; Situ, H.; Chehal, N. K.; Hultin, P. G.; Hein, J. E., Real-time HPLC-MS reaction progress monitoring using an automated analytical platform. *Reac. Chem. Eng.* **2017,** *2*, 309-314.
(11) Gross, E.; Shu, X.-Z.; Alayoglu, S.; Bechtel, H. A.; Martin, M. C.; Toste, F. D.; Somorjai, G. A., In situ IR and X-ray high spatial-resolution microspectroscopy measurements of multistep organic transformation in flow microreactor catalyzed by Au nanoclusters. *J. Am. Chem. Soc.* **2014,** *136*, 3624.
(12) Moore, J. S.; Jensen, K. F., "Batch" kinetics in flow: online IR analysis and continuous control. *Angew. Chem. Int. Edit.* **2014,** *53*, 470-473.
(13) Cao, E.; Brett, G.; Miedziak, P. J.; Douthwaite, J. M.; Barrass, S.; McMillan, P. F.; Hutchings, G. J.; Gavriilidis, A., A micropacked-bed multi-reactor system with in situ Raman analysis for catalyst evaluation. *Catal. Today* **2017,** *283*, 195-201.
(14) Cherkasov, N.; Bai, Y.; Expósito, A. J.; Rebrov, E. V., OpenFlowChem–a platform for quick, robust and flexible automation and self-optimisation of flow chemistry. *Reac. Chem. Eng.* **2018,** *3*, 769-780.

(15) Jensen, K. F., Flow Chemistry—Microreaction technology comes of age. *AIChE J.* **2017,** *63*, 858-869.
(16) Goodell, J. R.; McMullen, J. P.; Zaborenko, N.; Maloney, J. R.; Ho, C.-X.; Jensen, K. F.; Porco Jr, J. A.; Beeler, A. B., Development of an automated microfluidic reaction platform for multidimensional screening: reaction discovery employing bicyclo [3.2. 1] octanoid scaffolds. *J, Org. Chem.* **2009,** *74*, 6169-6180.
(17) Perera, D.; Tucker, J. W.; Brahmbhatt, S.; Helal, C. J.; Chong, A.; Farrell, W.; Richardson, P.; Sach, N. W., A platform for automated nanomole-scale reaction screening and micromole-scale synthesis in flow. *Science* **2018,** *359*, 429-434.
(18) Reizman, B. J.; Wang, Y.-M.; Buchwald, S. L.; Jensen, K. F., Suzuki-Miyaura cross-coupling optimization enabled by automated feedback. *Reac. Chem. Eng.* **2016,** *1*, 658-666.
(19) Holmes, N.; Akien, G. R.; Savage, R. J. D.; Stanetty, C.; Baxendale, I. R.; Blacker, A. J.; Taylor, B. A.; Woodward, R. L.; Meadows, R. E.; Bourne, R. A., Online quantitative mass spectrometry for the rapid adaptive optimisation of automated flow reactors. *Reac. Chem. Eng.* **2016,** *1*, 96-100.
(20) Holmes, N.; Akien, G. R.; Blacker, A. J.; Woodward, R. L.; Meadows, R. E.; Bourne, R. A., Self-optimisation of the final stage in the synthesis of EGFR kinase inhibitor AZD9291 using an automated flow reactor. *Reac. Chem. Eng.* **2016,** *1*, 366-371.
(21) Cortés-Borda, D.; Kutonova, K. V.; Jamet, C.; Trusova, M. E.; Zammattio, F.; Truchet, C.; Rodriguez-Zubiri, M.; Felpin, F.-X., Optimizing the Heck–Matsuda reaction in flow with a constraint-adapted direct search algorithm. *Org. Process Res. Dev.* **2016,** *20*, 1979-1987.
(22) Sans, V.; Porwol, L.; Dragone, V.; Cronin, L., A self optimizing synthetic organic reactor system using real-time in-line NMR spectroscopy. *Chem. Sci.* **2015,** *6*, 1258-1264.
(23) Reizman, B. J.; Jensen, K. F., Simultaneous solvent screening and reaction optimization in microliter slugs. *Chem. Commun.* **2015,** *51*, 13290-13293.
(24) Fitzpatrick, D. E.; Battilocchio, C.; Ley, S. V., A novel internet-based reaction monitoring, control and autonomous self-optimization platform for chemical synthesis. *Org. Process Res. Dev.* **2015,** *20*, 386-394.
(25) Bédard, A.-C.; Adamo, A.; Aroh, K. C.; Russell, M. G.; Bedermann, A. A.; Torosian, J.; Yue, B.; Jensen, K. F.; Jamison, T. F., Reconfigurable system for automated optimization of diverse chemical reactions. *Science* **2018,** *361*, 1220-1225.
(26) Schweidtmann, A. M.; Clayton, A. D.; Holmes, N.; Bradford, E.; Bourne, R. A.; Lapkin, A. A., Machine learning meets continuous flow chemistry: Automated optimization towards the Pareto front of multiple objectives. *Chem. Eng. J.* **2018,** *352*, 277-282.
(27) Cortés-Borda, D.; Wimmer, E.; Gouilleux, B.; Barré, E.; Oger, N.; Goulamaly, L.; Peault, L.; Charrier, B.; Truchet, C.; Giraudeau, P., An autonomous self-optimizing flow reactor for the synthesis of natural product carpanone. *J, Org. Chem.* **2018,** *83*, 14286-14299.
(28) Mateos, C.; Nieves-Remacha, M. J.; Rincón, J. A., Automated platforms for reaction self-optimization in flow. *Reac. Chem. Eng.* **2019,** *4*, 1536-1544.
(29) Jeraal, M. I.; Holmes, N.; Akien, G. R.; Bourne, R. A., Enhanced process development using automated continuous reactors by self-optimisation algorithms and statistical empirical modelling. *Tetrahedron* **2018,** *74*, 3158-3164.
(30) Galvanin, F.; Cao, E.; Al-Rifai, N.; Gavriilidis, A.; Dua, V., A joint model-based experimental design approach for the identification of kinetic models in continuous flow laboratory reactors. *Comput. Chem. Eng.* **2016,** *95*, 202-215.
(31) Galvanin, F.; Barolo, M.; Bezzo, F., Online model-based redesign of experiments for parameter estimation in dynamic systems. *Ind. Eng. Chem. Res.* **2009,** *48*, 4415-4427.
(32) Galvanin, F.; Macchietto, S.; Bezzo, F., Model-based design of parallel experiments. *Ind. Eng. Chem. Res.* **2007,** *46*, 871-882.
(33) Franceschini, G.; Macchietto, S., Anti-correlation approach to model-based experiment design: application to a biodiesel production process. *Ind. Eng. Chem. Res.* **2008,** *47*, 2331-2348.

(34) Franceschini, G.; Macchietto, S., Validation of a model for biodiesel production through model-based experiment design. *Ind. Eng. Chem. Res.* **2007,** *46*, 220-232.
(35) McMullen, J. P.; Jensen, K. F., Rapid determination of reaction kinetics with an automated microfluidic system. *Org. Process Res. Dev.* **2011,** *15*, 398-407.
(36) Reizman, B. J.; Jensen, K. F., An automated continuous-flow platform for the estimation of multistep reaction kinetics. *Org. Process Res. Dev.* **2012,** *16*, 1770-1782.
(37) Cruz Bournazou, M.; Barz, T.; Nickel, D.; Lopez Cárdenas, D.; Glauche, F.; Knepper, A.; Neubauer, P., Online optimal experimental re-design in robotic parallel fed-batch cultivation facilities. *Biotechnol. Bioeng.* **2017,** *114*, 610-619.
(38) Quaglio, M.; Waldron, C.; Pankajakshan, A.; Cao, E.; Gavriilidis, A.; Fraga, E. S.; Galvanin, F., An online reparametrisation approach for robust parameter estimation in automated model identification platforms. *Comput. Chem. Eng.* **2019,** *124*, 270-284.
(39) Schaber, S. D.; Born, S. C.; Jensen, K. F.; Barton, P. I., Design, execution, and analysis of time-varying experiments for model discrimination and parameter estimation in microreactors. *Org. Process Res. Dev.* **2014,** *18*, 1461-1467.
(40) Waldron, C.; Pankajakshan, A.; Quaglio, M.; Cao, E.; Galvanin, F.; Gavriilidis, A., An autonomous microreactor platform for the rapid identification of kinetic models. *Reac. Chem. Eng.* **2019,** *4*, 1623-1636.
(41) Hunter, W. G.; Reiner, A. M., Designs for discriminating between two rival models. *Technometrics* **1965,** *7*, 307-323.
(42) Box, G. E.; Hill, W. J., Discrimination among mechanistic models. *Technometrics* **1967,** *9*, 57-71.
(43) Buzzi-Ferraris, G.; Forzatti, P.; Emig, G.; Hofmann, H., Sequential experimental design for model discrimination in the case of multiple responses. *Chem. Eng. Sci.* **1984,** *39*, 81-85.
(44) Buzzi-Ferraris, G.; Forzatti, P., A new sequential experimental design procedure for discriminating among rival models. *Chem. Eng. Sci.* **1983,** *38*, 225-232.
(45) Box, G. E.; Hunter, W. G. *Sequential design of experiments for nonlinear models*; Wisconsin Univ Madison: 1963.
(46) Box, G. E.; Lucas, H., Design of experiments in non-linear situations. *Biometrika* **1959,** *46*, 77-90.
(47) Echtermeyer, A.; Amar, Y.; Zakrzewski, J.; Lapkin, A., Self-optimisation and model-based design of experiments for developing a C–H activation flow process. *Beilstein J. Org. Chem.* **2017,** *13*, 150-163.
(48) Bard, Y., *Nonlinear Parameter Estimation*. Academic Press: New York, 1974.
(49) Miao, H.; Xia, X.; Perelson, A. S.; Wu, H., On identifiability of nonlinear ODE models and applications in viral dynamics. *SIAM review* **2011,** *53*, 3-39.
(50) Brendel, M.; Bonvin, D.; Marquardt, W., Incremental identification of kinetic models for homogeneous reaction systems. *Chem. Eng. Sci.* **2006,** *61*, 5404-5420.
(51) Karalashvili, M.; Marquardt, W.; Mhamdi, A., Optimal experimental design for identification of transport coefficient models in convection–diffusion equations. *Comput. Chem. Eng.* **2015,** *80*, 101-113.
(52) Kun, K. A.; Kunin, R. In *The pore structure of macroreticular ion exchange resins*, Journal of Polymer Science Part C: Polymer Symposia, 1967; Wiley Online Library: 1967; pp 1457-1469.
(53) Kunin, R.; Meitzner, E. F.; Oline, J. A.; Fisher, S. A.; Fisher, N., Characterization of Amberlyst 15. *Ind. Eng. Chem. Prod. RD.* **1962,** *1*, 140-144.
(54) Pereira, C. S. M.; Pinho, S. P.; Silva, V. M. T. M.; Rodrigues, A. E., Thermodynamic equilibrium and reaction kinetics for the esterification of lactic acid with ethanol catalyzed by acid ion-exchange resin. *Ind. Eng. Chem. Res.* **2008,** *47*, 1453-1463.
(55) Lee, M.-J.; Chou, P.-L.; Lin, H.-M., Kinetics of synthesis and hydrolysis of ethyl benzoate over Amberlyst 39. *Ind. Eng. Chem. Res.* **2005,** *44*, 725-732.
(56) Pipus, G.; Plazl, I.; Koloini, T., Esterification of benzoic acid in microwave tubular flow reactor. *Chem. Eng. J.* **2000,** *76*, 239-245.
(57) Buzzi-Ferraris, G.; Manenti, F., Kinetic models analysis. *Chem. Eng. Sci.* **2009,** *64*, 1061-1074.

(58) Kallinikos, L. E.; Papayannakos, N. G., Fluid dynamic characteristics of a structured bed spiral mini-reactor. *Chem. Eng. Sci.* **2007,** *62*, 5979-5988.
(59) Moonen, R.; Alles, J.; Ras, E.-j.; Harvey, C.; Moulijn, J. A., Performance testing of hydrodesulphurization catalysts using a single pellet string reactor. *Chem. Eng. Technol.* **2017,** *40*, 2025-2034.
(60) Kallinikos, L. E.; Papayannakos, N. G., Intensification of hydrodesulphurization process with a structured bed spiral mini-reactor. *Chem. Eng. Process.* **2010,** *49*, 1025-1030.
(61) Kallinikos, L. E.; Papayannakos, N. G., Operation of a miniscale string bed reactor in spiral form at hydrotreatment conditions. *Ind. Eng. Chem. Res.* **2007,** *46*, 5531-5535.
(62) Müller, A.; Ludwig, M.; Arlit, M.; Lange, R., Evaluation of reactor concepts for the continuous production of fine chemicals using the selective hydrogenation of cinnamaldehyde over palladium catalysts. *Catal. Today* **2015,** *241*, 214-220.
(63) Gierman, H., Design of laboratory hydrotreating reactors: scaling down of trickle-flow reactors. *Appl. Catal.* **1988,** *43*, 277-286.
(64) Tidona, B.; Desportes, S.; Altheimer, M.; Ninck, K.; von Rohr, P. R., Liquid-to-particle mass transfer in a micro packed bed reactor. *Int. J. Heat Mass Tran.* **2012,** *55*, 522-530.
(65) Pöpken, T.; Götze, L.; Gmehling, J., Reaction kinetics and chemical equilibrium of homogeneously and heterogeneously catalyzed acetic acid esterification with methanol and methyl acetate hydrolysis. *Ind. Eng. Chem. Res.* **2000,** *39*, 2601-2611.
(66) Nelder, J. A.; Mead, R., A simplex method for function minimization. *Comput. J.* **1965,** *7*, 308-313.
(67) Antony, J., *Design of Experiments for Engineers and Scientists*. 2 ed.; Elsevier Science: Amsterdam, 2014.

For Table of Contents Only